# Exploring fMRI data for periodic signal components

Lars Kai Hansen, Finn Årup Nielsen and Jan Larsen

Informatics and Mathematical Modelling

Technical University of Denmark B321

DK-2800 Lyngby, DENMARK

Correspondence:

Tel: (+45) 4525 3889, Fax: (+45) 4587 2599

email: lkh@imm.dtu.dk

**Keywords**: Exploratory, fMRI, periodic signals, Bayesian framework

**Abstract**

We use a Bayesian framework to detect periodic components in fMRI data. The resulting detector is sensitive to periodic components with a flexible number of harmonics and with arbitrary amplitude and phases of the harmonics. It is possible to detect the correct number of harmonics in periodic signals even if the fundamental frequency is beyond the Nyquist frequency. We apply the signal detector to locate regions that are highly affected by periodic physiological artifacts, such as cardiac pulsation.

# 1 Introduction

In fMRI experiments we may want to local detect periodic components in the local hemodynamic activity. Much attention has been devoted to estimate the confounding signals generated by pulsatory activity at the cardiac frequency. The approaches range from simple digital filters [1] to sophisticated adaptive techniques based on the complex k-space MR signal [6], both methods are based on external monitoring of the cardiac activity. Dagli et al. concluded that regions near vessels have reduced sensitivity for detection of activation because of the signal variance induced by cardiac pulsation [2]. The typical acquisition frequencies (TR $\sim 3-4$ sec) in whole brain data sets preclude direct spectral filtering. Even for rapid acquisition single slice data sets the cardiac signal will have higher harmonics at frequencies beyond the Nyquist limit.

The quest for periodic components can be formulated as a local test for the presence of a periodic signal with flexible number of harmonics and basic frequency against a null-hypothesis under which the signal is white noise. We will review a Bayesian framework below that allows calculation of relative probabilities of such competing hypotheses; this framework was first applied in the context of fMRI data analysis in [5].

The Bayesian framework is of interest in this context because it gives a more complete picture of the interplay between the null hypothesis and relevant alternatives and the framework has an embedded quantitative statement of the a priori knowledge that enters the formulation of hypotheses. Our approach is a Bayesian generalization of the so-called general linear model used frequently in fMRI analysis, see e.g., [4]; the main generalization is that we can eliminate the unknown amplitudes and phases of the harmonics as well as the noise variance, which in turn allows us to operate the general linear model as an explorative tool.

Frank et al. [3] recently reviewed a Bayesian framework for signal detection in fMRI data. Here we expand on the application of the Bayesian framework based on so-called *conjugate priors* in the context of periodic component detection.

## 2 Bayes' Theory

We will be focus on models of the local hemodynamic activity in a region or as in this exposition, a single pixel. Let $\mathbf{y}$ be a fMRI signal measured at times $t = 1, ..., T$, and represented as a $T \times 1$ vector with components $\mathbf{y}(t)$. The signal is modeled as a sum of harmonic components of the form,

$$\widehat{\mathbf{y}}(t) = \sum_{k=1}^{K} \mathbf{x}_k(t)\mathbf{b}_k \tag{1}$$

where $\mathbf{x}_k(t)$ is a set of periodic "basis functions". $\mathbf{b}$ is a set of $K$ linear coefficients quantifying the content of signal of the given periodicity in the local hemodynamic activity. Introducing the $T \times K$ matrix with components $\mathbf{X}(t, k) \equiv \mathbf{x}_k(t)$ the linear model can be written in matrix form

$$\widehat{\mathbf{y}} = \mathbf{X}\mathbf{b} \tag{2}$$

In an fMRI experiment we expect that the actual measurement deviates from the "ideal" model output by various noise contributions that we will represent by a random white noise process so that $\mathbf{y}(t) = \widehat{\mathbf{y}}(t) + \mathbf{n}(t)$ where $\mathbf{n}(t)$ is assumed zero mean normal with unknown variance ($\sigma^2$).

The basis functions will be chosen as $\mathbf{x}_{2k-1}(t) = \sin(kw_0t), \mathbf{x}_{2k}(t) = \cos(kw_0t), \quad k = 1, ..., K$, where $w_0$ is the fundamental frequency of the signal. By including a linear combination of both sines and cosines, we can generate harmonics with arbitrary phase relations. Note that a model with $\kappa$ frequencies has $K = 2\kappa$ basis functions, hence a $2\kappa$ dimensional coefficient vector $\mathbf{b}$.

A fundamental problem posed by Eq. (2) and the definitions above is that the model order $K$, the fundamental frequency $w_0$, and the noise variance $\sigma^2$ are unknown. Here we will develop a Bayesian scheme that we allow us to make inferences about these parameters, independent of the amplitude and phase of the harmonics and independent of the noise variance. This is achieved by invoking a simple, yet flexible prior distribution

of these parameters so that we may eliminate these parameters by explicit integration. In particular we will aim at estimating the probability $P(w_0, K|\mathbf{y})$ of the "hypothesis" specified by $w_0, K$, using Bayes' theorem,

$$P(w_0, K|\mathbf{y}) = \frac{P(\mathbf{y}|w_0, K)P(w_0, K)}{P(\mathbf{y})}, \tag{3}$$

where $P(\mathbf{y}|w_0, K)$ is the likelihood function, $P(w_0, K)$ is the prior probability, whereas $P(\mathbf{y})$ is a normalization constant.

For a fixed set of parameters $\mathbf{b}, \sigma^2$ we can use Eq. (2) to establish the likelihood function, i.e., the probability density of the observations given the parameters,

$$P(\mathbf{y}|\sigma^2, \mathbf{b}, \mathbf{X}, K) = \left(\frac{1}{2\pi\sigma^2}\right)^{T/2} \exp\left(-\frac{1}{2\sigma^2}(\mathbf{y} - \mathbf{X}\mathbf{b})^2\right). \tag{4}$$

Since, however, $\mathbf{b}, \sigma^2$ are unknown too we need to eliminate them using a *prior distribution* $P(\mathbf{b}, \sigma^2)$ which quantifies the general knowledge we have on the domain and which potentially depends on the given basis set and model order,

$$\begin{aligned} P(\mathbf{y}|w_0, K) &= \int d\sigma^2 \int d\mathbf{b} P(\mathbf{b}, \sigma^2) P(\mathbf{y}|\sigma^2, \mathbf{b}, \mathbf{X}, K) \\ &= \int d\sigma^2 \int d\mathbf{b} P(\mathbf{b}, \sigma^2) \left(\frac{1}{2\pi\sigma^2}\right)^{T/2} \exp\left(-\frac{(\mathbf{y} - \mathbf{X}\mathbf{b})^2}{2\sigma^2}\right). \end{aligned} \tag{5}$$

We will use the principle of *congugate priors* to establish a convenient prior $P(\mathbf{b}, \sigma^2)$. The subsequent analysis is described comprehensively in most textbooks on Bayesian data analysis, see e.g. [7] for a particularly clear treatment. The idea is to employ a prior density so that the posterior (proportional to the product of the prior and the likelihood, c.f., eq. (3)) is of the same form as the prior but with "updated", i.e., data dependent, parameters. The conjugate prior for the above linear model with additive gaussian noise is the so-called *normal-inverse-gamma* or NIG$(a, d, \mathbf{m}, \mathbf{V})$, distribution,

$$P(\mathbf{b},\sigma^2|a,d,K,\mathbf{m},\mathbf{V}) = \frac{(a/2)^{d/2}(\sigma^2)^{-(d+K+2)/2}}{(2\pi)^{K/2}|\mathbf{V}|^{1/2}\Gamma(d/2)} \exp\left(-(\mathbf{b}-\mathbf{m})'(2\sigma^2\mathbf{V})^{-1}(\mathbf{b}-\mathbf{m}) - \frac{a}{2\sigma^2}\right). \tag{6}$$

The new (hyper-) parameters $d, a, \mathbf{m}, \mathbf{V}$ have the following meaning. The marginal prior distribution of $\mathbf{b}$,

$$\begin{aligned} P(\mathbf{b}|a,d,K,\mathbf{m},\mathbf{V}) &= \int d\sigma^2 P((\mathbf{b},\sigma^2|m,K) \\ &= \frac{(a/2)^{-K/2}\Gamma((d+K)/2)}{(2\pi)^{K/2}|\mathbf{V}|^{1/2}\Gamma(d/2)} \left(1+(\mathbf{b}-\mathbf{m})'(a\mathbf{V})^{-1}(\mathbf{b}-\mathbf{m})\right)^{-(d+K+2)/2} \end{aligned} \tag{7}$$

is a multivariate $t$-distribution with mean $\mathbf{m}$ and covariance determined by $(a/(d-2))\,\mathbf{V}$. This distribution is unimodally centered at $\mathbf{m}$, with heavier "tails" than a normal distribution, see figure 1. The marginal prior distribution of $\sigma^2$ is given by

$$P(\sigma^2|a,d) = \frac{(a/2)^{-d/2}(\sigma^2)^{-(d+2)/2}}{\Gamma(d/2)} \exp\left(-a/(2\sigma^2)\right). \tag{8}$$

Hence an inverse gamma distribution[1] of mean $a/(d-2),\ d>2$.

The next step of the inference is then to set the parameters of the prior. In general we prefer to give the parameters values so that they have minimal influence on results. In particular, we should check that for long time series their effects should vanish completely.

The prior mean of the noise variance can, e.g., be set to the observed signal variance, $a/(d-2) = \sigma_y^2 \equiv \mathbf{y}'\mathbf{y}/T$, meaning that we do not expect a noise variance larger than the total observed variance. Further we will let $d=3$ leading to a prior as shown in figure 1, this choice of $d$ is the smallest integer for which the prior noise variance is finite, hence, a "weak" prior. We will not express any prior knowledge about the mean amplitude of the periodic components, hence, $\mathbf{m}=\mathbf{0}$. The form of the prior covariance structure is chosen for simplicity to be $\mathbf{V} = v\mathbf{1}$, where $\mathbf{1}$ is a unit matrix. The parameter $v$ will be

[1] i.e., $1/\sigma^2$ is gamma distributed

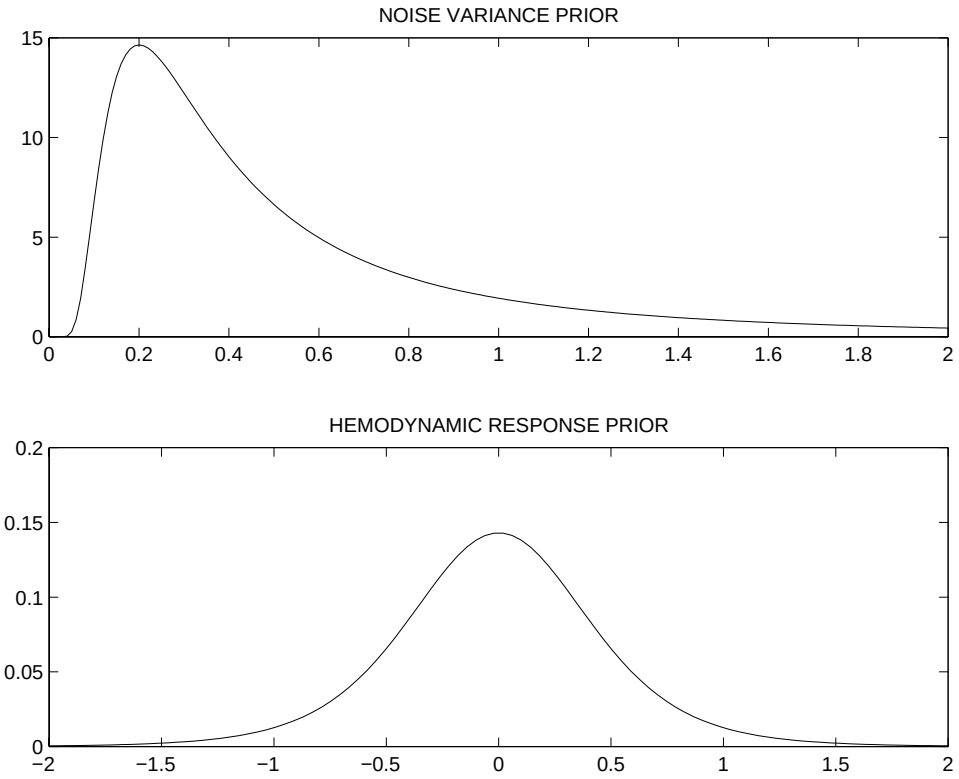


Figure 1: Visualization of the prior distribution of the noise variance and the the hemodynamic impulse response. The upper panel shows the inverse gamma distribution of the noise variance parameter, while the lower panel shows the prior distribution of a hemodynamic impulse response parameter. The distribution is wider than a Gaussian of the same variance. These priors were first used for analyzing fMRI hemodynamics in [5]

determined essentially by data by the following argument. The prior variance of the fitted signal $\hat{\mathbf{y}}$, is given by

$$\langle \hat{\mathbf{y}}' \hat{\mathbf{y}} \rangle_{\text{prior}} / T = \mathsf{Tr}[\mathbf{X}\mathbf{X}' \langle \mathbf{b}\mathbf{b}' \rangle_{\text{prior}} / T] = (va/(d-2)) \mathsf{Tr}[\mathbf{X}\mathbf{X}']/T \tag{9}$$

As above, for the noise variance hyperparameter selection, we can let variance be equal to the variance of the measured signal, i.e., let $v = 1/\mathsf{Tr}[\mathbf{X}\mathbf{X}']/T$.

Comparing Eqs. (4) and (6) we see that by conjugacy they are of the same exponential form, so when we multiply them together, the integrand in Eq. (5) is again an NIG

distribution, hence the integral is simply the NIG normalization integral, thus we find

$$P(\mathbf{y}|w_0, K) = \left(\frac{|\mathbf{V}_\mathrm{P}|a^d}{|\mathbf{V}|(a_P)^{d_P}\pi^T}\right)^{1/2} \frac{\Gamma(d_P/2)}{\Gamma(d/2)}, \tag{10}$$

with the following definitions

$$\mathbf{V}_P^{-1} = \mathbf{V}^{-1} + \mathbf{X}'\mathbf{X}, \tag{11}$$

$$\mathbf{m}_P = \mathbf{V}_P(\mathbf{V}^{-1}\mathbf{m} + \mathbf{X}'\mathbf{y}), \tag{12}$$

$$a_P = a + \mathbf{m}'\mathbf{V}^{-1}\mathbf{m} + \mathbf{y}'\mathbf{y} - \mathbf{m}'_P\mathbf{V}_P^{-1}\mathbf{m}_P, \tag{13}$$

$$d_P = d + T. \tag{14}$$

Using our specifications of the prior parameters we obtain the simplification

$$\mathbf{V}_P^{-1} = v\mathbf{1} + \mathbf{X}'\mathbf{X}, \tag{15}$$

$$\mathbf{m}_P = \mathbf{V}_P\mathbf{X}'\mathbf{y}, \tag{16}$$

$$a_P = (T+1)\sigma_y^2 - \mathbf{y}'\mathbf{X}\mathbf{V}_P\mathbf{X}'\mathbf{y}, \tag{17}$$

$$d_P = 3 + T. \tag{18}$$

We can see explicitly that the influence of the prior choice of $a$ and $d$ is weak for $T \gg 1$, because the prior contributions are of order one relative to $T$ in Eqs. (17) and (18) respectively.

Testing the above linear system hypotheses, a natural null-hypothesis is that the signal is gaussian noise of unknown variance. The corresponding probability density $P(\mathbf{y}|0)$ is given by the $\mathbf{X} = \mathbf{0}$ limit of the above expressions.

The probabilities of the set of complete set of hypotheses (parameterized by $w_0$ and $K$) including the null-hypothesis are then given by

$$
\begin{aligned}
P(w_0, K|\mathbf{y}) &= \frac{P(\mathbf{y}|w_0, K)}{P(\mathbf{y}|0) + \sum_{w_0,K} P(\mathbf{y}|w_0, K)} \\
P(0|\mathbf{y}) &= \frac{P(\mathbf{y}|0)}{P(\mathbf{y}|0) + \sum_{w_0,K} P(\mathbf{y}|w_0, K)}
\end{aligned} \tag{19}
$$

# 3 Evaluation on simulated and real fMRI data

## 3.1 Simulation experiments

In order to illustrate the viability of the Bayesian approach for exploring time series for periodic components we have set up a simulation experiment. A signal was created by mixing a periodic signal (two harmonics) and gaussian white noise signal of the same standard deviation. In Figure 2 we show the true and the noisy signals, in the case the fundamental frequency is lower than the Nyquist frequency. The middle panel shows the signal reconstructed from the maximum a posteriori parameters ($\mathbf{m}_P$). In the lower panel of Figure 2 we show the Bayesian probabilities for hypotheses with $\kappa = 1, ..., 10$ frequencies, which is strongly focused at the true value of $\kappa = 2$, even in the presence of sizable noise contamination. In Figure 3 we show a similar setup as in Figure 2, except now the fundamental frequency is beyond the Nyquist. In this case the periodic signal is aliased to appear as a low-frequency signal, but importantly we may still detect its presence, and can still correctly detect that it consists of two harmonics.

## 3.2 fMRI experiment

A single fMRI slice holding $128 \times 128$ pixels and cutting through primary visual cortex was acquired with a time interval between successive scans of TR = 333 msec. A window of $M = 82 \times 68$ pixels covering all of the brain of the particular slice was extracted for this analysis. This sampling frequency is high enough to allow faithful representation of the heart signal. Visual stimulation in the form of a flashing annular checkerboard

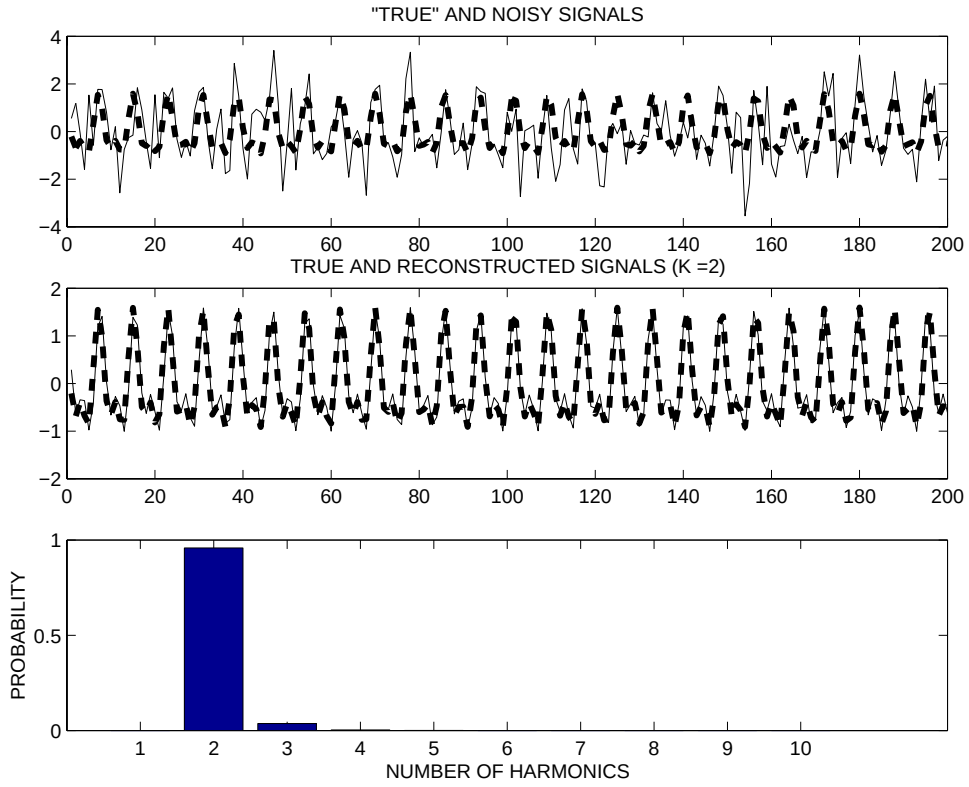


Figure 2: Simulation experiment created to illustrate the ability of the Bayesian approach for picking up the correct model order. The upper panel shows the true periodic signal (heavy dashed line) composed by the fundamental and the second harmonic (of relative amplitude 0.6). The noisy signal is obtained by adding gaussian noise of the same standard deviation as the "signal". The middle panel shows the true signal (heavy dashed line) and the maximum a posteriori reconstructed signal. The lower panel shows the probability of having $\kappa = 1, ..., 10$ harmonics. As expected, this probability is strongly peaked at the true value $\kappa = 2$.

pattern was interleaved with periods of fixation. A run consisting of 30 scans of fixation, 31 scans of stimulation, and 60 scans of post-stimulus fixation was repeated 10 times. The data set was acquired by Dr. Egill Rostrup at the Danish Center for Magnetic Resonance Research.

In each voxel we test the hypotheses: The white noise nul hypothesis, and a set of hypotheses parameterized by fundamental frequencies and number of components. Figure 4 shows the distribution of the pixel-wise most probable number of frequencies ($\kappa$).

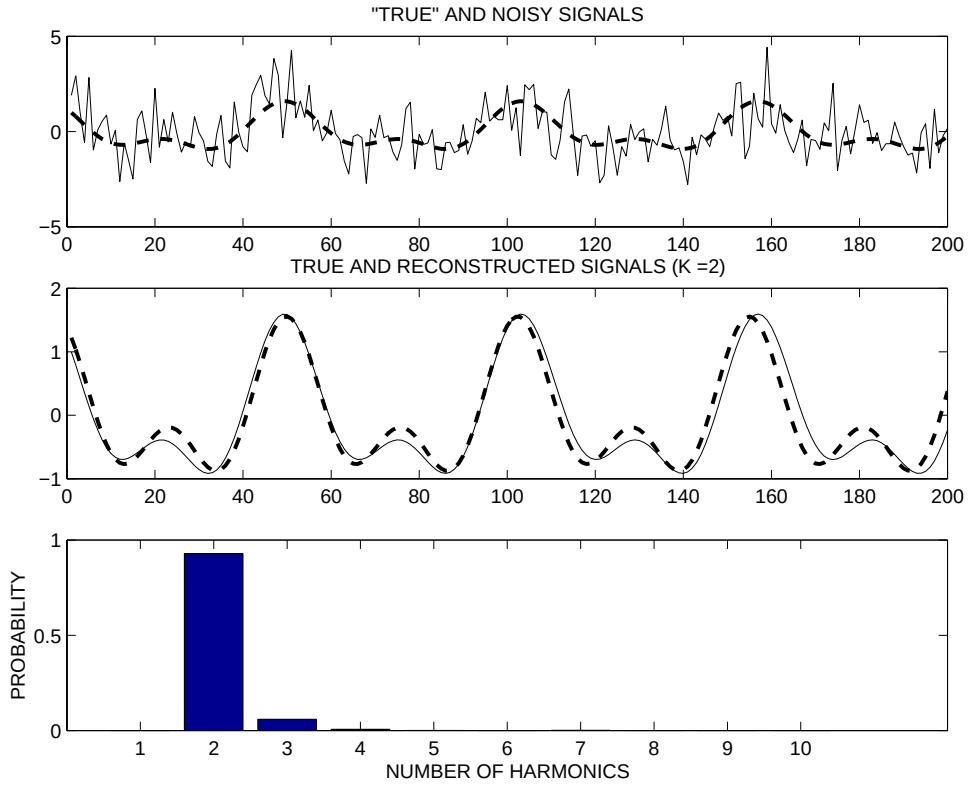


Figure 3: Simulation experiment created to show the ability of the Bayesian approach for picking up the correct model order even when the fundamental frequency is undersampled. The upper panel shows the true periodic signal (heavy dashed line) composed by the fundamental and the second harmonic (of relative magnitude $0.6$). The angular frequency is $w_0^{\text{true}} = 6.4$, this signal is aliased to appear low-frequency. The noisy signal is obtained by adding noise of the same standard deviation as the signal. The middle panel shows the true signal (heavy dashed line) and the maximum a posteriori reconstructed signal. The lower panel shows the probability of having $\kappa = 1 - 10$ harmonics. As expected, this probability is strongly peaked at the true value $\kappa = 2$.

Black pixels are assigned to the null-hypothesis, whereas the brightest pixels have four harmonics. Two locations are singled out for further analysis. The "vessel" pixel has four harmonics and is dominated by a high-frequency component corresponding to the cardiac frequency. The "primary visual" pixel has only one low-frequency component. In Figure 5 we show the analysis of the primary visual area hemodynamic activity. This region has

a strong positive stimulus response corresponding to a very low-frequency component. In Figure 6 we show the analysis of the vessel pixel. This region is dominated by cardiac pulsation and is well approximated by the reconstructed MAP high-frequency signal.

# 4 Conclusion

We have outlined a Bayesian framework for signal detection in noisy linear systems. We used weak conjugate priors and as a result we obtain closed form expressions for the relative probabilities over competing hypotheses. Formulating a model based on periodic signals with a variable number of harmonics, we obtain a periodic component detector, this detector can detect periodic signals with arbitrary amplitude and phase relations between the harmonics, and was shown able to detect the correct number of harmonics even if the fundamental frequency is beyond the Nyquist frequency.

# Acknowledgments

We thank Dr. Egill Rostrup for access to the fMRI data set used for illustration in this paper. Our work is funded by the Danish Research Councils through the THOR Center for Neuroinformatics, the EU Commission through project MAPAWAMO, and by the US National Institutes of Health Human Brain Project grant P20 MH57180 "Spatial and Temporal Patterns in Functional Neuroimaging".

# References

[1] B. Biswal, E.A. DeYoe, J.S. Hyde, Reduction of Fluctuations in fMRI Using Digital Filters, *Magnetic Resonance in Medicine 35* (1996) 107-113.

[2] M.S. Dagli, J.E. Ingeholm and J.V. Haxby, Localization of Cardiac-Induced Signal Change in fMRI, *NeuroImage 9* (1999) 407-415.

[3] L.R. Frank, R.B. Buxton, and E.C. Wong, Probabilistic Analysis of Functional Magnetic Resonance Imaging Data, *Magnetic Resonance in Medicine 39* (1998) 132-148.

[4] K.J. Friston, Statistical Parametric Mapping and other analyses of functional imaging data, in: Eds. A.W. Toga and J.C. Mazziota, *Brain Mapping, The Methods* (Academic Press, San Diego 1996) 363-396 .

[5] L.K. Hansen, A. Purutshotham, S.-G. Kim, Testing Competing Hypotheses about fMRI data *in press.*

[6] X. Hu, T.H. Lee, T. Parish, and P.E. Erhard, Retrospective Estimation and Correction of Physiological Fluctuation in Functional MRI, *Magnetic Resonance in Medicine 34* (1995) 201-212.

[7] A. Ohagan: *Bayesian Inference.* Kendall's Advanced Theory of Statistics. Vol 2B. (The University Press, Cambridge, 1994).

# Captions

1. Visualization of the prior distribution of the noise variance and the the hemodynamic impulse response. The upper panel shows the inverse gamma distribution of the noise variance parameter, while the lower panel shows the prior distribution of a hemodynamic impulse response parameter. The distribution is wider than a Gaussian of the same variance. These priors were first used for analyzing fMRI hemodynamics in [5]

2. Simulation experiment created to illustrate the ability of the Bayesian approach for picking up the correct model order. The upper panel shows the true periodic signal (heavy dashed line) composed by the fundamental and the second harmonic (of relative amplitude 0.6). The noisy signal is obtained by adding gaussian noise of the same standard deviation as the "signal". The middle panel shows the true signal (heavy dashed line) and the maximum a posteriori reconstructed signal. The lower panel shows the probability of having $\kappa = 1, ..., 10$ harmonics. As expected, this probability is strongly peaked at the true value $\kappa = 2$.

3. Simulation experiment created to show the ability of the Bayesian approach for picking up the correct model order even when the fundamental frequency is undersampled. The upper panel shows the true periodic signal (heavy dashed line) composed by the fundamental and the second harmonic (of relative magnitude 0.6). The angular frequency is $w_0^{\text{true}} = 6.4$, this signal is aliased to appear low-frequency. The noisy signal is obtained by adding noise of the same standard deviation as the signal. The middle panel shows the true signal (heavy dashed line) and the maximum a posteriori reconstructed signal. The lower panel shows the probability of having $\kappa = 1 - 10$ harmonics. As expected, this probability is strongly peaked at the true value $\kappa = 2$.

4. A single slice holding $128 \times 128$ pixels and cutting through primary visual cortex

was acquired with a time interval between successive scans of TR = 333 msec. A window of $M = 82 \times 68$ pixel covering all of the brain of the particular slice was extracted for this analysis. The sampling frequency of this acquisition mode is high enough to allow faithful representation of the heart signal. Visual stimulation in the form of a flashing checkerboard pattern was interleaved with periods of fixation. A run consisting of 30 scans of fixation, 30 scans of stimulation, and 60 scans of post-stimulus fixation was repeated 10 times, here we analyze a single run. The figure shows the distribution of pixel-wise most probable model order ($\kappa$). Black pixels are assigned to the null-hypothesis, while the brighter pixels have up to four harmonics. Two locations are singled out for further analysis. The "vessel" pixel and the "primary visual" pixel. The most probable frequency is high corresponding to cardiac pulsation in the former and low, corresponding to the presentation frequency of the stimulus in the latter region.

5. Analysis of the "primary visual" pixel of Figure 4. This region has a strong positive activation trace and the optimal fundamental frequency is $\sim 0.03$ Hz. The measured signal is represented by the thin line, the MAP reconstructed signal is rendered with the heavy line.

6. Analysis of the "vessel" pixel of Figure 4. This region consists mainly of a high-frequency cardiac pulsation signal, well described by the periodic signal model with four harmonics.

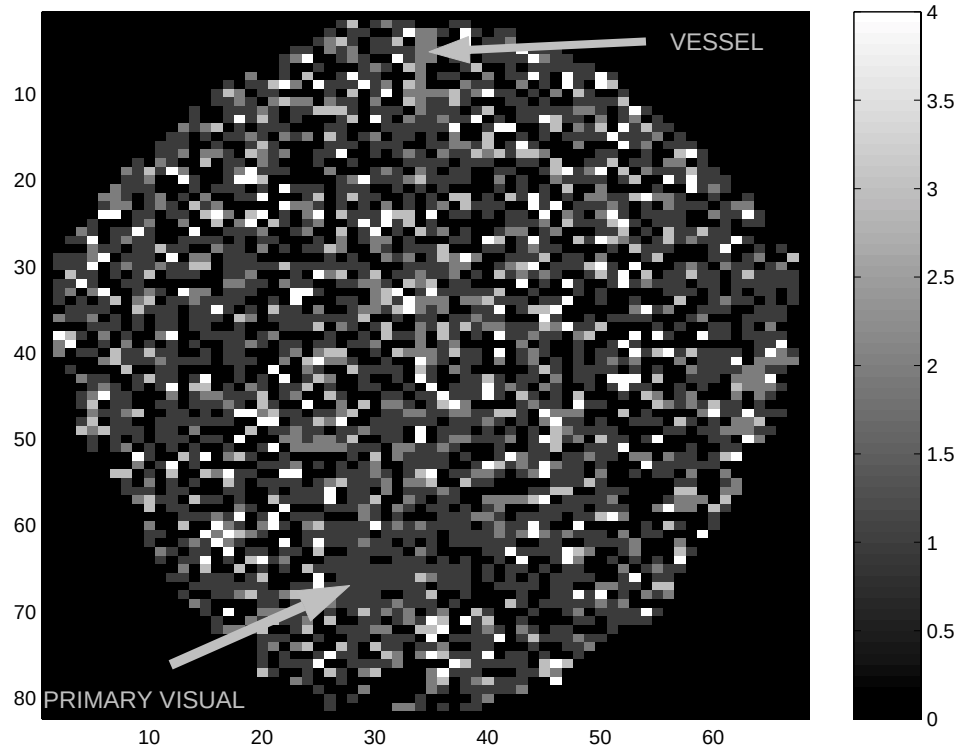


Figure 4: A single slice holding $128 \times 128$ pixels and cutting through primary visual cortex was acquired with a time interval between successive scans of TR $= 333$ msec. A window of $M = 82 \times 68$ pixel covering all of the brain of the particular slice was extracted for this analysis. The sampling frequency of this acquisition mode is high enough to allow faithful representation of the heart signal. Visual stimulation in the form of a flashing checkerboard pattern was interleaved with periods of fixation. A run consisting of 30 scans of fixation, 30 scans of stimulation, and 60 scans of post-stimulus fixation was repeated 10 times, here we analyze a single run. The figure shows the distribution of pixel-wise most probable model order ($\kappa$). Black pixels are assigned to the null-hypothesis, while the brighter pixels have up to four harmonics. Two locations are singled out for further analysis. The "vessel" pixel and the "primary visual" pixel. The most probable frequency is high corresponding to cardiac pulsation in the former and low, corresponding to the presentation frequency of the stimulus in the latter region.

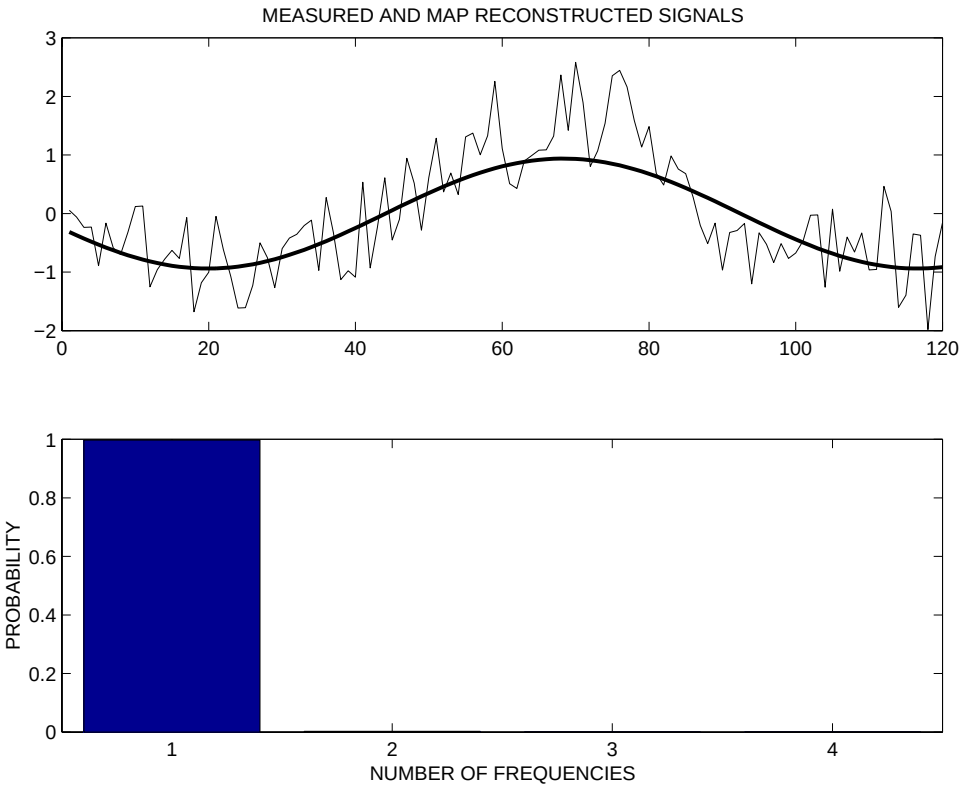


Figure 5: Analysis of the "primary visual" pixel of Figure 4. This region has a strong positive activation trace and the optimal fundamental frequency is $\sim 0.03$ Hz. The measured signal is represented by the thin line, the MAP reconstructed signal is rendered with the heavy line.

.

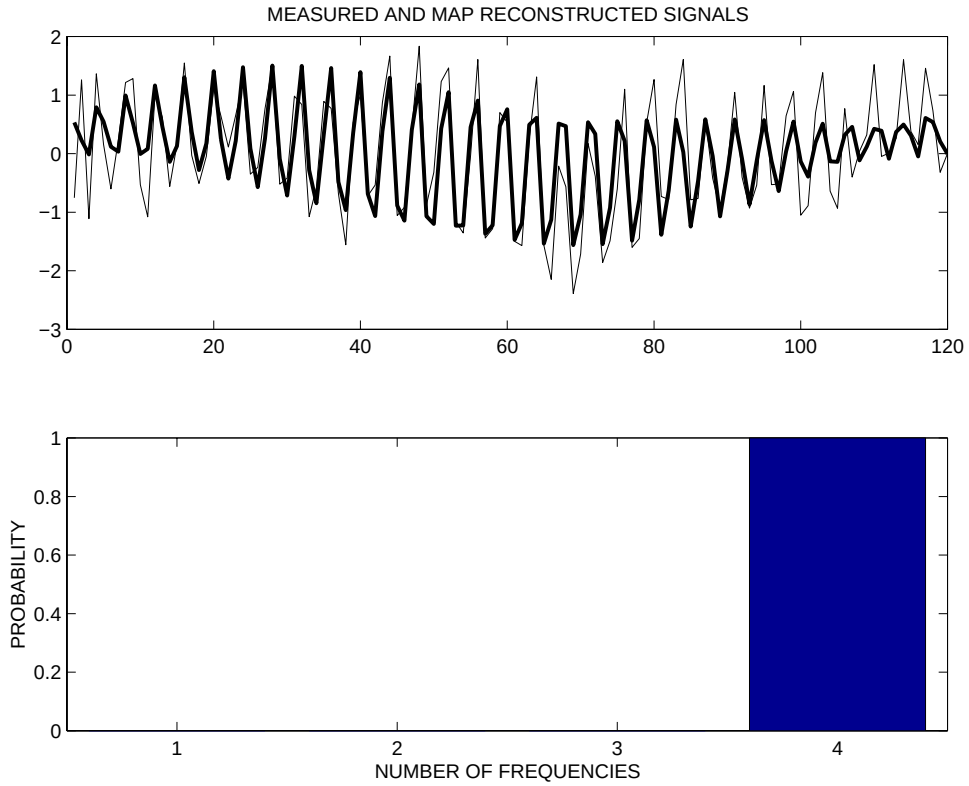


Figure 6: Analysis of the "vessel" pixel of Figure 4. This region consists mainly of a high-frequency cardiac pulsation signal, well described by the periodic signal model with four harmonics.